Project Number: MQP NAB MP11

Surface Independent Friction Force Calibration

A Major Qualifying Project Report

Submitted to the Faculty

Of

WORCESTER POLYTECHNIC INSTITUTE

In partial fulfillment of the requirements for the

Degree of Bachelor of Science

By

Taylor Esformes

April 29, 2010

____

N.A. Burnham, Advisor

Abstract

Lateral Force Microscopy (LFM) is a powerful technique for imaging nanoscale structures by measuring friction. Data regarding the magnitude of the nanoscale friction force is difficult to obtain. In order to measure this force, it is necessary to calibrate the cantilever for lateral forces. We mathematically derived a new model for lateral force calibration. The model was tested in order to verify its consistency. This new calibration method may be an attractive alternative to existing lateral force calibration methods.

Acknowledgments

I would like to thank Professor Nancy Burnham for her guidance, patience and invaluable assistance during this project. I would also like to thank Professor Gibson of the Biochemistry Department for the use of his equipment and supplies, and the Sigma Xi research organization for funding this research.

Table of Contents

Abstract 2
Acknowledgments 3
Table of Figures 5
2 Lateral Force Calibration Through The Years: A Literature Review 8
I. Atomic-Scale Friction of a Tungsten Tip on a Graphite Surface: The Mate Method 10
II. Calibration of Frictional Forces in Atomic Force Microscopy: The Ogletree Method 11
III. Force Calibration in Lateral Force Microscopy: The Cain Method 12
IV. An Improved Wedge Calibration Method for Lateral Force in Atomic 13
Force Microscopy: The Varenberg Method 13
V. Direct Force Balance Method for Atomic Force Microscopy Lateral Force 14
Calibration: The Asay and Kim Method 14
VI. A New Lateral Force Calibration Method and General Guidelines for Optimization: The Cannara Method 15
VII. Lateral Force Calibration of an Atomic Force Microscope with a Diamagnetic Levitation Spring System: The Li-Kim-Rydberg Method 16
VIII. Surface-Independent Friction Force Calibration 17
3 Experimental Approach 19
I. The Atomic Force Microscope 19
II. Materials 24
III. Computer Analysis 24
4 Results 28
5 Conclusions 32
Appendix A: Mathematical Derivation of the Experimental Model 34
Appendix B: The Micropipette Puller 41

Table of Figures

Figure 2-1: An LFM image of a graphite polycrystal ……………………………………11

Figure 2-2: A Topographic image used in the Ogletree Calibration Method ……..……12

Figure 2-3: The free body diagram used to derive the Asay and Kim Method ….…..…15

Figure 3-4 Diagram of an AFM scanner head ……………………………….…..….… 19

Figure 3-2: Raw data from a typical LFM scan …………………………….………….. 22

Figure 3-3: Graph of Lateral Force vs. LFM voltage …………………………….….….23

Figure 3-4: Flowchart of data processing procedure ……………………….....………25

Figure 4-1: A computer generated data graph ……..……………………….……...…. 27

Figure 4-2: A graph of calibration factor as a function of set point ………………………29

Figure 4-3: Scatter plot of calibration factors for cantilevers of different length……….. 30

Figure A-2: Coordinate System of Cantilever ……………………………………….....33

Figure A-1: Coordinate System of Scanner Motion ………………………………………33

Figure A-4: 2nd Rotation about the P axis ………………………………………………… 34

Figure A-3: 1st Rotation about the J axis ………………………………………………….. 34

Figure A-5: Forces acting on the cantilever tip …………………………………………… 35

Figure A-6: Graph of Lateral Force versus LFM voltage …………………………………37

Figure B-1: The WPI PUL-1 Micropipette Puller ………………………………………… 40

Figure B-2: A micropipette, properly loaded in the micropipette puller …………………42

1 Introduction

The Atomic Force Microscope (AFM) is an incredibly important tool in the study of nanostructures. As the study of physics begins to advance into the blurred realm between the classical and quantum worlds, it becomes increasingly vital that imaging technology advances with it. The study of biology, physics, and materials all depend on the ability to properly image nanoscale phenomena. The purpose of this project is to further advance the techniques used in Lateral Force Microscopy, a closely related branch of AFM.

The first LFM was a relatively primitive device; the cantilever was a thin tungsten wire, and the scanning head did not possess any of the software or hardware-based error correction systems that modern researchers use. Yet, even this primitive device was able to image both periodic and single-atom phenomena in a piece of graphite crystal.

LFM is an extremely promising branch of physics, though it suffers from some temporary flaws. Most important among these flaws is the difficulty with obtaining quantitative data on the force of friction at the nanoscale. By increasing the accuracy of friction force measurements, the new calibration method developed in this report will allow researchers to take reliable quantitative data on the material properties of a wide variety of surfaces.

This report will begin with a review of the relevant literature on the topic of lateral force calibration. The experimental procedure will then be described in full, followed by a discussion of the results and some concluding thoughts. In Appendix A, there is a

detailed explanation of the mathematical model derived for this project. Appendix B is a tutorial on the use of the PUL-1 Micropipette Puller.

2 Lateral Force Calibration Through The Years: A Literature Review

When it was developed in 1986 by the team of Binnig, Gerber, and Quate, the Atomic Force Microscope (AFM) sparked a revolution in material science, biology, and physics. Binnig had already been recognized for his contributions to nanoscience that year when he earned the 1986 Nobel Prize in Physics for the invention of the Scanning Tunneling Microscope, another invaluable tool in the study of nanoscale phenomena. Before the invention of AFM, microscopic resolution of non-conductive samples was limited by the frequency of light used to illuminate the sample. The resolution of a microscope is governed by the Abbe formula, which states that

$$D = \frac{\lambda}{NA},$$

where D is the diffraction limit of the microscope, is the wavelength of light, and NA is the numerical aperture of the objective, a function of the aperture angle and the index of refraction of the medium filling the space between the lens and objective. For most optical microscopes, the theoretical resolution limit is about 200 nm. The most common way of overcoming this obstacle is the use of high energy ultraviolet radiation as the light source.

Binnig avoided this issue by collecting topographical data in a novel way. Instead of collecting incident photons from the surface of the sample, his AFM lightly brushed the surface with a flexible gold cantilever with a sharp diamond tip at the end. He used a scanning tunneling microscope (STM) in order to measure cantilever deflection.

Nowadays, most AFMs have a self-contained laser to measure cantilever deflection. The back of the cantilever is coated in a reflective surface, usually gold or aluminum, to allow the laser to be focused on it. The reflected laser point hits a photodiode mounted on the scanner head, and the resultant voltage is recorded by a computer. The vertical deflection of the cantilever as it encounters topographical features can be measured is a function of this voltage, and the data thus collected are used to create a nanoscale image of the sample. The resolution limit of an AFM is primarily a function of the accuracy of the photodiode and the diameter of the tip used in imaging. The result of this advantage is that AFM is capable of resolutions on the order of a few angstroms. In fact, within one year of the invention of AFM, Mate et al. were able to use the AFM to detect single-atom phenomena on the surface of a sheet of graphite. They were able to accomplish this through the use of Lateral Force Microscopy.

LFM operates on many of the same principles as AFM, but measures frictional forces instead of topographical details. By measuring the torsional deflection of the cantilever, it is possible to calculate the force of friction between the sample and the cantilever. Measurement of the torsional deflection is made possible by using a quadrant photodiode. By using a photodiode with four sections, both the lateral and vertical deflections can be measured with excellent precision. However, in order to know quantitatively the force on the cantilever, it is necessary to establish a relationship between the angle of torsion and the force of friction. The multitudes of techniques for accomplishing this are known collectively as lateral force calibration methods. Mate's 1987 paper on lateral force calibration is the first attempt at a calibration method, though the goal of the paper was to detect single-atom friction phenomena on a crystalline

surface. His attempt to predict friction forces using macroscopic friction relations was ultimately incomplete, but Mate's work laid down the foundation for a new and rich field in physics, and the great abundance of literature his work inspired is the groundwork for this project.

I. Atomic-Scale Friction of a Tungsten Tip on a Graphite Surface: The Mate Method

The first calibration method, published in 1987, assumed that the macroscopic formula for friction applied to microscopic phenomena. The macroscopic friction relation is

$$F = N * \mu ,$$

Where F is the force of friction, N is the normal force and μ is the empirically measured coefficient of fiction. The experiment used to test this hypothesis is a simple cantilever, made from a tungsten wire being dragged across a grain of highly-oriented graphite polycrystal. Interestingly enough, the experimenters were able to detect the periodicity of the atoms on the surface of the sample, and the periodicity of the friction force due to the crystalline structure of the sample. The linear model of friction forces is a poor approximation, unfortunately; Mate speculates in his paper that the relationship between applied load and friction force is an exponential function, but is unable to offer further speculation.[2]

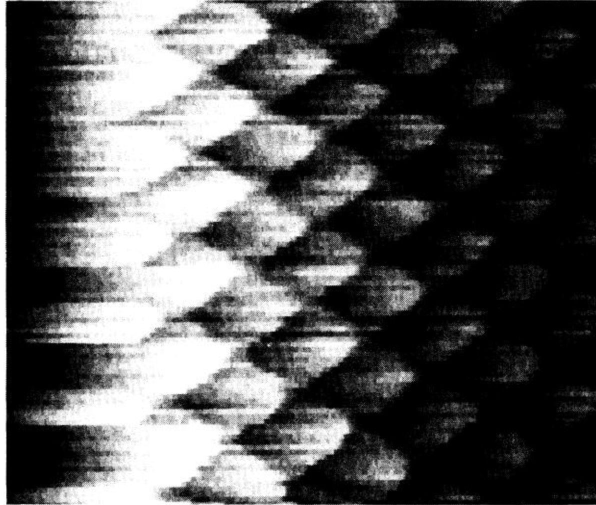

Figure 2-1: An LFM image of the graphite polycrystal surface used in the Mate experiment. The left-to-right fading effect is due to the lack of correction software available to compensate for distortion due to piezoelectric scanners.[2]

II. Calibration of Frictional Forces in Atomic Force Microscopy: The Ogletree Method

This method, published in 1996, is considered the standard method of lateral force calibration. The basic idea behind this method of lateral force calibration is to make repeated scans with the probe in question on an angled surface. During the scan, the experimenter measures the forces lateral and normal to the cantilever. The total lateral force is equal to the sum of the surface forces and the geometrical contribution of the cantilever, equal to the product of the load on the cantilever and the tangent of the surface's slope. By measuring the lateral force as a function of a known quantity like the applied load, the cantilever's lateral force constant can be calculated.

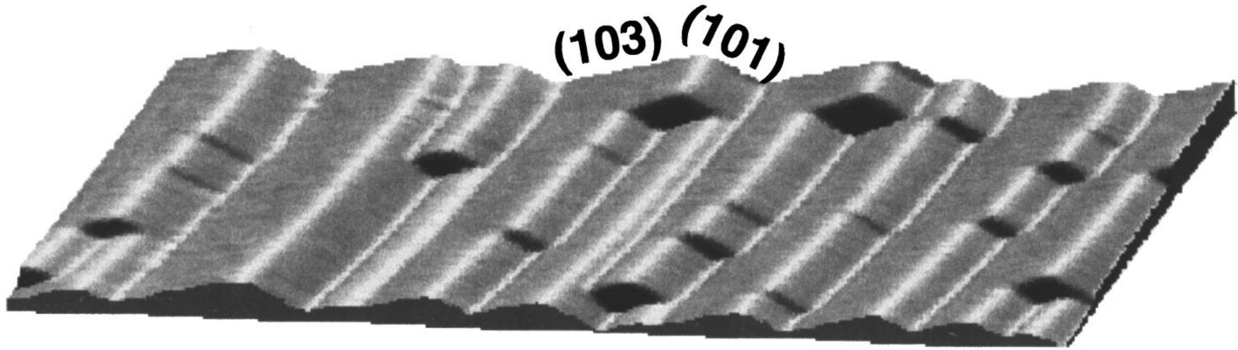

Figure2-2: A Topographic image of the strontium titanate surface used in the Ogletree Calibration Method. The (103) and (101) crystal facets used as the "wedge" are labeled as such. [3]

Ogletree's method requires the use of a special surface made from $SrTiO_{3,}$ strontium titanate. Strontium titanate has the unusual property of forming perfectly angled surfaces when treated with heat in an oxygen environment. It forms 12.5 and 14 degree facets spaced 10-100 nm apart, making them ideal for imaging under an AFM. Unfortunately, there are no manufacturers of lab quality strontium titanate samples; the material must be carefully cleaved by the experimenter. The Ogletree method also requires multiple scans with the cantilever in question, causing wear to the tip and possibly skewing results. These issues make the Ogletree method an inconvenient one for researchers. Soon after the publication of the original article, a flurry of work on lateral force calibration followed, with many researchers building upon the original wedge method calibration in order to improve its accuracy and efficiency.[3]

III. Force Calibration in Lateral Force Microscopy: The Cain Method

The Cain Method, published three years after Ogletree's paper, uses a computer model to describe the cantilevers. This approach allows the experimenter to find the Young's modulus of the cantilever, and therefore the lateral force constant. According to the model, the lateral force constant is equal to

$$k_\theta = h^2 k_{tot}(1 + \frac{y_c}{y}),$$

where h is the distance between the cantilever neutral axis and the sample, y is the vertical deflection, y_c is the lateral deformation of the cantilever-surface interface, and k_{tot} is the total stiffness, a function of the lateral contact stiffness k_{yc} (not the lateral force constant) and the vertical contact stiffness k_y, calculated thusly:

$$k_{tot} = (\frac{1}{k_y} + \frac{1}{k_{yc}})^{-1}.$$

The lateral contact stiffness can be calculated using data from the LFM friction loop, a graph of applied load versus friction in both scanning directions. The model requires, however, that the cantilever's normal force constant be known, along with its thickness. Measuring the thickness of a cantilever usually requires a Scanning Electron Microscope to be accurate, limiting the usefulness of the this method, but measuring the normal force constant of a cantilever is a simple process, done by measuring the resonant frequency of the cantilever and using the given geometry of the cantilever to analytically calculate the force constant.[4]

IV. An Improved Wedge Calibration Method for Lateral Force in Atomic Force Microscopy: The Varenberg Method

A 2002 paper by M. Varenberg et al. described an improved wedge method for lateral force calibration. Like all wedge methods, it involves scanning a sloped surface with the cantilever being calibrated. It improves on the Ogletree method most significantly by allowing the use of a commercially available grating as the sloped surface, in this case the TGF11 calibration sample. The TGF11 resembles a crystal with faces of orientation (100) and (111), forming two perfect 54.44 degree angles periodically along the surface. [5] However, the method shares with Ogletree the unfortunate need to conduct a large

number of scans with the cantilever in question, causing wear and decreasing resolution.

V. Direct Force Balance Method for Atomic Force Microscopy Lateral Force Calibration: The Asay and Kim Method

The Asay and Kim method for lateral force calibration follows a similar scheme to the Ogletree method. Again, the experimenter uses surfaces with facets of a known angle, and measures the forces on the cantilever as a function of deflection. The mathematical model used in this method assumes that the cantilever is at equilibrium at any point in the scan. Using the force-deflection curves already measured, the experimenter can calculate the lateral force on the cantilever as a function of the surface angle and the applied load, and from there calculate the lateral force constant, which is the merely the ratio of the lateral force to the lateral voltage signal at that point in the scan. It should be noted that the initial assumptions used to make this model have been demonstrated to be flawed. Specifically, the free-body diagrams used to derive the equilibrium conditions mischaracterized the direction of the lateral force on a cantilever tip and failed to take into account the force of friction across the surface. Nevertheless, this method has the advantage of minimizing tip wear, as it does not require repeated scans.[6]

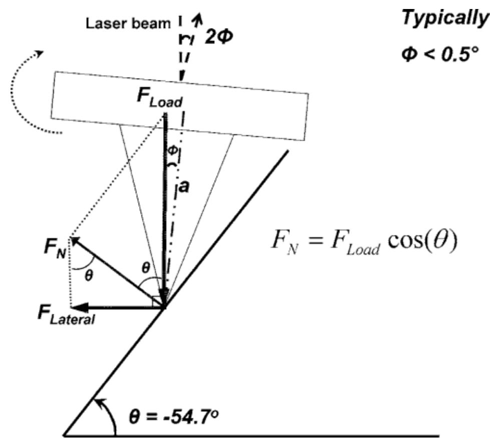

Figure 2-3: The free body diagram used to derive the Asay and Kim Method. Notice that the force of friction on the cantilever is not represented and that the lateral force is acting on the wrong location and in the wrong direction. [6]

VI. A New Lateral Force Calibration Method and General Guidelines for Optimization: The Cannara Method

The Cannara Method, also known as the “test probe” method, requires the use of two cantilevers. The probe in question is a cantilever of dimensions and coating as similar as possible to the one to be calibrated. A colloidal sphere is glued to the end of the test probe and the experimenter takes lateral force versus deflection data by running the probe over a surface featuring a 90 degree slope. The surface used in the Cannara paper was gallium arsenide, a fairly common semiconductor which cleaves at right angles. Cannara also performed a comparison of the test probe method and the wedge methods described above. An obvious advantage of the Cannara method crops up early on, as it becomes necessary to measure the normal force constant when using the wedge method but not when using the test probe method. However, the method also requires the use of a cantilever other than the one actually being used in the experiment, requiring that the experimenter assume that the cantilever manufacturing method is highly consistent.[7]

VII. Lateral Force Calibration of an Atomic Force Microscope with a Diamagnetic Levitation Spring System: The Li-Kim-Rydberg Method

Diamagnetism is the property of creating magnetic fields in opposition to an externally applied field. The Li-Kim-Rydberg method uses a diamagnetic lateral force calibrator, or DLFC, to act as a load cell for the measurement of the lateral force constant. The DLFC uses a sheet of graphite as its diamagnetic material. The geometry of the sheet ensures that air resistance and eddy current forces remain negligible by keeping the sheet as still as possible. The DLFC consists of four square magnets arranged in a square pattern, with the magnets having polarization opposite to that of their adjacent neighbors. A square layer of pyrolytic graphite levitates on top of the magnets at the center of the arrangement, rotated 45 degrees relative to the magnets. The spring constants of the oscillating system can be controlled by changing the distance between the magnets. The experimenter mounts the DLFC on the AFM stage and then scans a sample of interest that has been glued to the top of the graphite sheet. The feedback system is programmed to maintain a constant normal load on the cantilever, and the photodiode output is recorded versus the displacement of the sample. The lateral force constant is equal, in this case, to the partial derivative of the lateral force with respect to the photodiode output. While this method is certainly one of the most innovative, it does have the singular disadvantage of requiring that a complex device be constructed with great precision in order to keep the graphite sheet from destabilizing or giving false data.[8]

VIII. Surface-Independent Friction Force Calibration

The purpose of this project is to improve upon these methods of lateral force calibration by addressing the drawbacks that each of them suffer from. For example, the Carpick and Cannara methods do not actually calibrate the cantilever in question, but a close facsimile; the experimenter must assume that the manufacturing process for the cantilevers is consistent or the resultant data is useless. Although the Ogletree method does not technically suffer from this setback, the numerous scans required to complete the calibration usually require that a new cantilever be used in the actual experiment. Other methods, such as those put forth by Ogletree and Li, require rare and specialized equipment that limit their practicality. Methods such as the original Mate approach impose a certain algebraic form on the expression for the friction force, possibly causing difficulties in analysis later. The Asay and Kim method suffers from the particularly noticeable drawback of being based upon faulty assumptions about the nature and direction of the lateral force on the cantilever tip.

The method put forth in this report attempts to address all of these concerns. Only one cantilever is required for calibration, which can be performed *in situ* with equipment readily available to any LFM laboratory. No specialized surfaces or devices are required for this method, nor are there assumptions about the mathematical form of the friction force expression to deal with because the friction term is eliminated during the mathematical derivation of the model. Most importantly, the process can be completed with only one LFM scan, minimizing damage to the cantilever during calibration. The proposed method is a significant improvement on existing calibration techniques.

References

1. Binnig, G., Quate, C.F., Gerber, Ch. (1986). Atomic Force Microscope *Physical Review Letters,* **56**(9), 930-934.

2. Mate, C.M., McClelland, G.M., Erlandsson, R., & Chiang, S. (1987). Atomic Scale Friction of a Tungsten Tip on a Graphite Surface *Physical Review,* **59**(7), 1942-1946.

3. Ogletree, D.F., Carpick, R.W., Salmeron, M. (1996). Calibration of Frictional Forces in Atomic Force Microscopy *Review of Scientific Instruments* **67**(9), 3298-3306.

4. Cain, Robert G., Biggs, Simon., Page, Neil W., (2000) Force Calibration in Lateral Force Microscopy *Journal of Colloid and Interface Science* 227, 55-65

5. Varenberg, M., Etsion, I., Halperin, G. (2003). An improved Wedge Calibration Method for Lateral Force in Atomic Force Microscopy, *Review of Scientific Instruments* **74**(7), 3362-3367

6. Asay, David B., Kim, Seong H. (2006) Direct Force Balance Method for Atomic Force Microscopy Lateral Force Calibration *Review of Scientific Instruments,* **77**, 043903

7. Cannara, Rachel J., Eglin, Michael., Carpick, Robert W. (2006) Lateral Force Calibration in Atomic Force Microscopy: A New Lateral Force Calibration Method and General Guidelines for Optimization *Review of Scientific Instruments,* **77**,053701

8. Li, Q., Kim, K.-S., Rydberg, A. (2006) Lateral Force Calibration of an Atomic Force Microscope with a Diamagnetic Levitation Spring System *Review of Scientific Instruments,* **77**,065105

3 Experimental Approach

I. The Atomic Force Microscope

An Atomic Force Microscope (AFM) takes topographic images by measuring the deflection of a flexible cantilever moving across the surface of a sample. The AFM can achieve lateral resolution limited primarily by the diameter of the cantilever tip and a vertical resolution mostly limited by the sensitivity of the photodiode used in the scanner head.

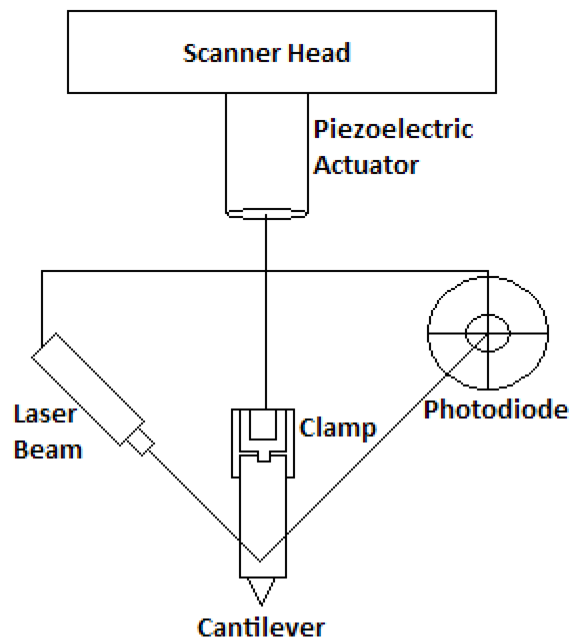

Figure 3-1 Diagram of an AFM scanner head

The cantilever is usually integrated a much larger silicon chip, which is fitted into a clamp and the loaded into the scanner. The clamp serves to keep the chip stationary, as a laser beam must be focused on the cantilever in order to take data from it. The cantilever is normally coated in a reflective substance such as gold or aluminum in order to properly reflect the laser.

The laser is reflected onto a photodiode, a device which creates a voltage across its poles when it is struck with light. When not scanning, the cantilever reflects the laser point directly into the center of the photodiode. When the cantilever encounters topography, however, it is deflected either upwards or downwards, and the laser point moves across the photodiode's surface accordingly. By shining more light on one part of the photodiode than another, a voltage differential is created. The computer can measure this signal with great precision; once the system is properly calibrated, the deflection of the cantilever can be calculated as a function of the LFM signal. A typical photodiode is divided into either two or four sections. A two-sectioned photodiode can measure the vertical deflection of the cantilever, but is useless for Lateral Force Microscopy. For LFM, we use a quadrant photodiode, capable of measuring both the vertical and lateral deflection of the cantilever.

AFM images can have an area of anywhere from a square micron all the way up to ten thousand square microns. In order to take images at such a small scale, a device is required that can cause the cantilever to oscillate across the sample surface with great precision. The scanner uses a piezoelectric tube to move the cantilever. Piezoelectric materials deform in the presence of an electric field due to reordering of the electrostatic domains in the material. The tube used by the scanner head is divided into four sections, with a strip of metal running on both the outside and the inside of the surface. When a voltage is applied across one of the sections, the electric magnetic field causes the tube to deflect in that direction, causing the cantilever to move as well. In order to guide the cantilever towards the correct part of the sample the scanner is equipped with a high-resolution camera underneath it and a highly precise computer-

based positioning stage. The scanner head itself also has a high-precision motorized vertical positioner.

The most basic component of any AFM is the cantilever. This is a flexible bar of silicon or silicon nitride, with an extremely sharp tip at the end which moves along the sample surface. They are typically 100-500 microns in length, with longer cantilevers corresponding to lower spring constants. Cantilevers come in two basic shapes, triangular and rectangular. Rectangular cantilevers are used in this report as they are easier to model mathematically. The normal force constant of a rectangular cantilever is

$$k_n = \frac{Ewt^3}{3L^3},$$

Where E is the Young's Modulus of the material, w is the width of the cantilever, t is the thickness and L is the length. If the width and thickness are not known, the equation can be stated in terms of the length of the cantilever, where

$$k_n = \frac{3EI}{L^3}\ .$$

E is, again, the Young's Modulus of the material, L is the length, and I is the moment of inertia. For a rectangular object, the moment of inertia is equal to

$$I = \frac{wt^3}{12}\ ,$$

where w is the width of the cantilever and t is the thickness.

Calculating the lateral force constant is a much more complicated matter, and is the purpose of this project. Nominally, the lateral force constant of a cantilever is expressed as

$$k_l = \frac{Gt^3w}{3Lh^2}.$$

In this expression:

- G is the shear modulus of the cantilever.
- T is the thickness of the cantilever.
- W is the width of the cantilever.
- L is the distance from the base of the cantilever to the base of the tip.
- H is the torsional moment arm of the cantilever, i.e., the distance from the twisting axis of the cantilever to the end of the tip. [1]

The mathematical basis for our model calculates the forces at the tip-sample interface as functions of surface angles, and averages them in order to disregard the contribution of the force of friction between the sample and tip. The final result of the model expresses the lateral force as

$$F_{lat} = k_n \, \Delta z \tan(\theta), \qquad (3\text{-}1)$$

a function of the surface angle θ, the normal force constant k_n, and the scanner's change in vertical position Δz, all quantities that can be easily measured (See Appendix A for the derivation of our model). The computer program used to process the data then correlates the LFM voltage data with the calculated lateral force at every point along the topography of the sample. Figure 1 is an example of a set of raw data images obtained by LFM.

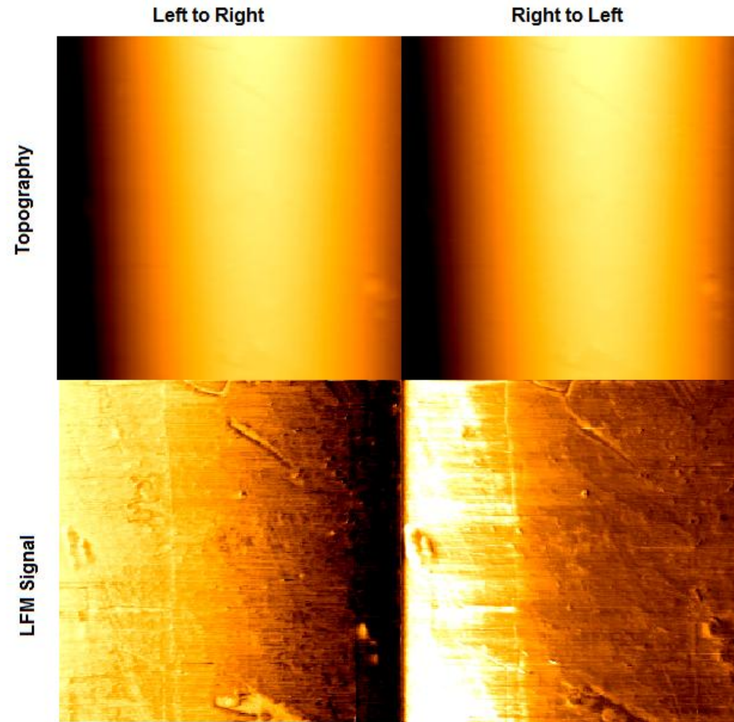

Figure 3-2: Raw data from a typical LFM scan. These images are converted into numeric arrays so that they can be analyzed by our computer program.

The data points take an approximately linear distribution on a graph of voltage versus force.

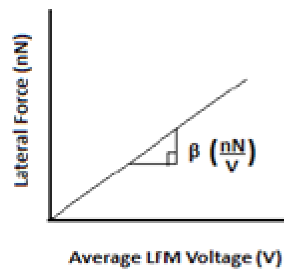

Figure 3-3: Graph of Lateral Force vs. LFM voltage

The slope of this line, i.e., the ratio of lateral force to LFM voltage, is known as the calibration factor β:

$$F_{lat} = \beta\, V_{LFM-AV} \qquad (3\text{-}2)$$

By combining Eq. 1 and Eq. 2, an expression for the calibration factor in terms of the measured data is reached:

$$\beta = \frac{k_n \, \Delta z \tan(\theta)}{V_{LFM-AV}} \qquad (3\text{-}3)$$

The computer program averages these calibration factors and determines an average lateral force constant for the cantilever.

II. Materials

The samples used for data collection are borosilicate glass micropipettes. These glass tubes are commonly used in biology for injecting cells with electrolyte solutions. In order to be used in the lab, micropipettes must be drawn to a fine point using a micropipette puller. The device clamps down on both ends of a micropipette and applies heat to the center of the tube. The clamping arms are spring loaded in order to pull the micropipette apart once it has been heated. The result is two symmetrical glass cones with a tip diameter ranging from 100nm to a micron. The processed micropipettes are mounted on glass slides with a cyanoacrylate-based adhesive and allowed to cure overnight. Micropipettes have several advantages with regards to LFM data collection. Unlike the methods put forth by Ogletree[2] or Li[3], the samples used in this experiment are easy to find and quite inexpensive. When pulled correctly, a micropipette can achieve an extremely low radius of curvature around the tip, allowing the LFM to scan a broader range of cantilever angles without having to scan a large area of the micropipette tip. They are also fairly robust and are easily replaced in the event of tip breakage. A pulled micropipette is extremely smooth on the nanoscale, resulting in a cleaner LFM signal and more precise data.

III. Computer Analysis

A custom computer program was written in order to quickly analyze the data collected from the LFM. During an LFM scan, four different images are made; two topographic images and two LFM signal images, one each going from right to left and from left to right. This allows the computer to calculate the calibration factor using a greatly simplified mathematical form of the expression for lateral force. (See Appendix A for a full mathematical derivation of this lateral force calibration method.) LFM images can be converted to a 256 by 256 array of numbers for ease of computation; in reality, the array of numbers is what the LFM actually collects, and the image is extrapolated from it, not the other way around. The computer can determine the slope between two adjacent points on the topographical image and then correlate that data with the corresponding LFM signal data in order to find a value for the cantilever's calibration factor. The resultant data points are plotted on a graph of LFM signal vs. cantilever deflection. The 65536, or 256^2, data points form an approximately linear distribution, the slope of which is the average lateral force calibration factor of the cantilever, within a certain margin of error, of course.

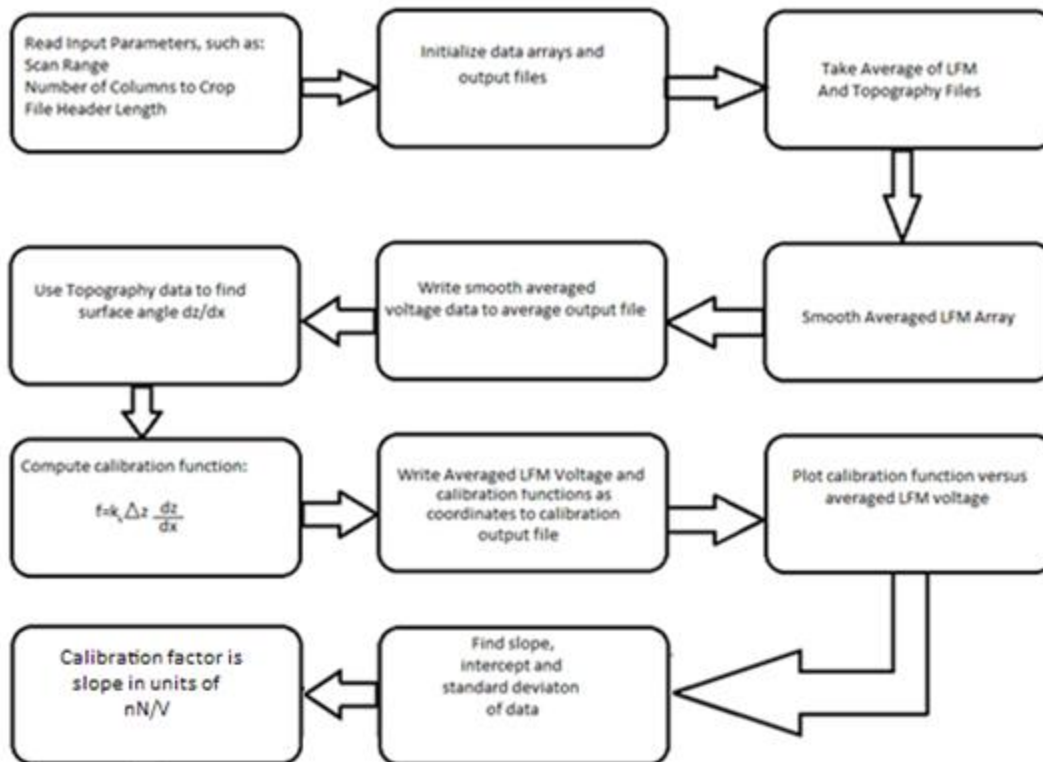

Figure 3-4: Flowchart of mathematical analysis program data processing procedure

References:

1. Cannara, Rachel J., Eglin, Michael., Carpick, Robert W. (2006) Lateral Force Calibration in Atomic Force Microscopy: A New Lateral Force Calibration Method and General Guidelines for Optimization *Review of Scientific Instruments,* **77**,053701
2. Ogletree, D.F., Carpick, R.W., Salmeron, M. (1996). Calibration of Frictional Forces in Atomic Force Microscopy Review of Scientific Instruments **67**(9), 3298-3306.
3. Li, Q., Kim, K.-S., Rydberg, A. (2006) Lateral Force Calibratoin of an Atomic Force Microscope with a Diamagnetic Levitation Spring System Review of Scientific Instruments, **77**,065105

4 Results

The method for lateral force calibration outlined in this report relies on a derived expression for the lateral force in terms of easily measured quantities,

$$\overline{F_{lat}} = k_n \Delta z \tan(\theta) ,$$

where k is the normal force constant, delta-z is the vertical response from the cantilever, and theta is the surface angle. This equation makes several testable predictions about the behavior of the lateral force data. The first prediction made by the model is that the lateral force is proportional to the magnitude of the normal force for any given surface angle. In other words, a graph of lateral force voltage v.s. normal force should demonstrate an approximately linear distribution.

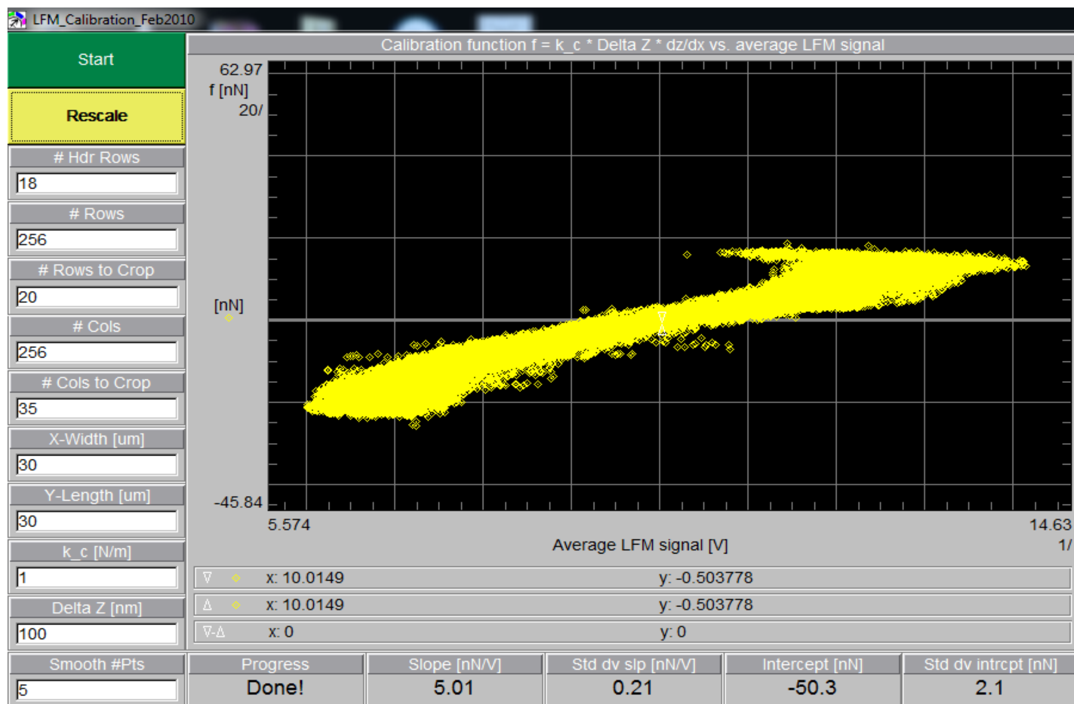

Figure 4-1: A computer generated graph correllating LFM signal and calibration function. The slope of this graph is the calibration factor.

Fig. 1 is a typical graph generated by the custom data processing program used in this experiment.The data collected followed the linear distribution fairly consistently; while the great majority of the data followed a linear pattern, clumps of outlier points caused by static recorded during the imaging process, particularly the "lobes" at the top and bottom ends of the grpah, added uncertainty to the calculation of the calibration factor. Nevertheless, the linear distribution of the data was highly pronounced, supporting the model's hypothesis.

The full equations governing the calculations of calibration factor are:

$$\begin{aligned} \overline{F_{lat}} &= F_{load_z} \tan(\theta) \\ &= k_n \Delta z \tan(\theta) \\ &= \beta V_{AV-LFM} \, . \end{aligned}$$

At first glance, it would appear that since the lateral force is equal in magnitude to the sum of the surface-tip interactions, one could control the calibration factor by increasing or decreasing the set point of the scanner head; the set point controls the force value which the scanner regards as "zero position" for the cantilever's topographical measurements. Such an obvious flaw in the theory would render the method useless, but the apparent problem is easily solved by reexamining the terms of the expression. The lateral force is obviously a linear function of the delta-z factor and the surface angle. However, it is also equal to the sum of the x-component of the surface-tip interactions, which are in turn equal to the magnitude of the force corresponding to the voltage value of the set point. A quick transitive reshuffling reveals that the vertical action of the scanner head, the delta-z factor, is in fact a linear function of the set point. In other words, as the set point increases, both the delta-z and the magnitude of the lateral force increase by the same amount.

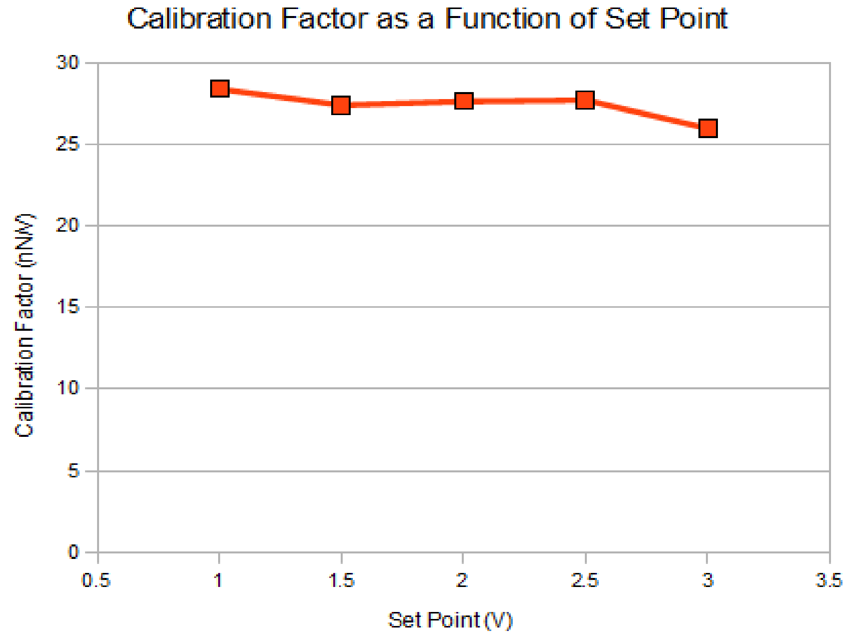

Figure 4-2: A graph of calibration factor as a function of set point

As can be seen in Fig. 3, the calibration factor data collected are not uniform, but they are spread across very a narrow range of values, due to a small amount of experimental error. This error is most likely due to wear on the cantilever, as the cantilevers used in this experiment had been previously used for several months, unusual for a research-grade cantilever. It was decided that since the scope of this project does not include taking detailed quantitative measurements of the calibration factor, but instead taking broader quantitative data samples, it was not necessary to use brand-new cantilevers, and a significant cost could be avoided.

Similarly, the model predicts that a change in the cantilever's torsional force constant will necessarily change the lateral force calibration factor; the equation for the torsional force constant of a rectangular cantilever is

$$k = \frac{G\,t^3\,w}{3\,L\,h^2},$$

where G is the Young's Modulus of the material, and w, t, L and h are width, thickness, length and torsional moment arm length, respectively. The easiest way to test this prediction is the

change the geometry of the cantilevers in use. The torsional force constant is highly sensitive to changes in the tip geometry, so the lateral force calibration factor should be just as sensitive to such changes.

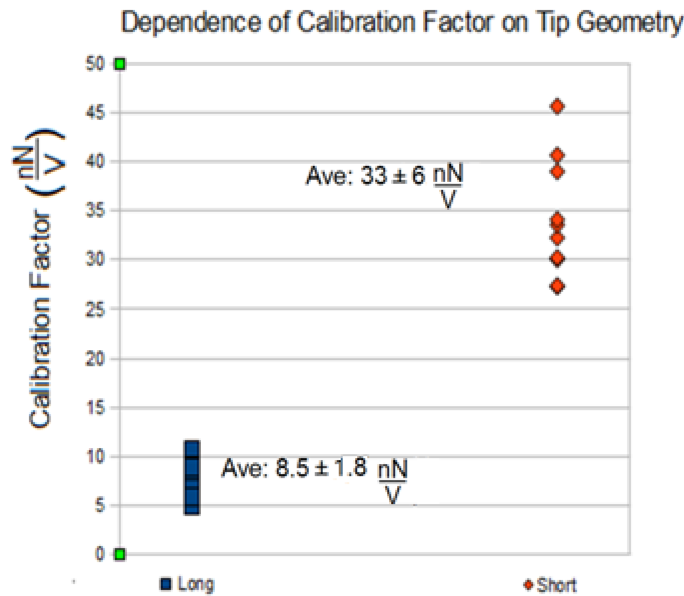

Figure 4-3: Scatter plot of calibration factors for cantilevers of different length

In tests of cantilevers with similar composition and different lengths, the data show a clear relationship between calibration factor and cantilever geometry, with shorter cantilevers posessing consistently higher calibration factors. Figure 2 is a graph of the distribution of calibration factors collected from two cantilevers of different length. The two data clusters are quite far apart, as even a small change in geometry can have a profound effect on lateral force calibration factor.

5 Conclusions

This project began with a simple mathematical derivation which indicated that the torsional force on a cantilever should be equal in magnitude to the sum of the surface-tip interactions it encountered. Appendix A is an overview of the current form of this derivation. After three years of study, the concept was tested experimentally. This project focused on qualitatively investigating the plausibility of the theory. This was to be accomplished by identifying the behavior that the model predicted and testing those predictions in the laboratory. The three main predictions of the Surface-Independent Lateral Force Calibration model are the following:

1. That the data set correlating LFM signal and Lateral Force should fit a linear distribution.
2. That the slope of that line, the lateral force calibration factor, should be unaffected by changes in set point.
3. That the lateral force calibration factor should change as a result of a change in cantilever geometry.

While it may be too early to claim confirmation of the theories outlined here, the data that have been collected and analyzed points to our model as an excellent step forward towards achieving the ultimate goal of this project; developing a quick and simple method of lateral force calibration with enough accuracy to be useful in a research laboratory without the use of specialized samples, conducting multiple scans or using a cantilever other than the one being calibrated. The next step will be to conduct quantitative testing of the model, comparing the accuracy of established calibration methods versus our approach. The theoretical error of the standard wedge methods

stands at approximately 4.2% [1], leaving only a small margin for improvement, but the main advantage of our calibration method is its ease of use, speed and that it generates very little tip wear.

References:

1. Cannara, Rachel J., Eglin, Michael., Carpick, Robert W. (2006) Lateral Force Calibration in Atomic Force Microscopy: A New Lateral Force Calibration Method and General Guidelines for Optimization *Review of Scientific Instruments,* **77**,053701

Appendix A: Mathematical Derivation of the Experimental Model

The derivation of the model used to analyze the LFM data collected begins by setting up the appropriate coordinate systems. The first is the coordinate system of the scanner head's motion.

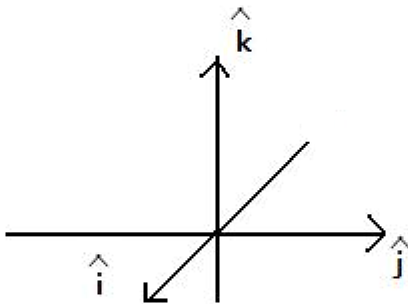

Figure A-1: Coordinate System of Scanner Motion

This coordinate system corresponds to the standard I-J-K system commonly used in physics. In this case:

- $\hat{\imath}$ is the unit vector pointing out of the paper. It is perpendicular to the long axis of the cantilever.
- $\hat{\jmath}$ is the horizontal unit vector. It is nominally parallel to the long axis of the cantilever.
- $\hat{k}$ is the vertical unit vector. It is nominally perpendicular to the plane of the surface.

The second coordinate system pertains to the cantilever itself:

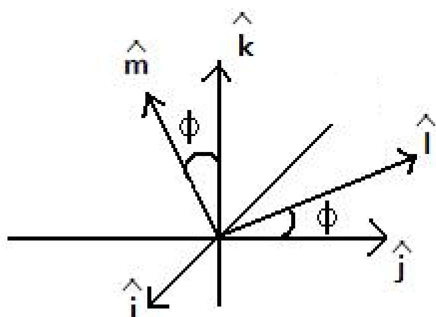

Figure A-2: Coordinate System of Cantilever

This coordinate system results from a rotation about the $\hat{\imath}$ axis. In this case:

- $\hat{l}$ is the unit vector pointing along the length of the cantilever.
- $\hat{m}$ is the unit vector pointing along the length of the tip. It is perpendicular to the $\hat{l}$ unit vector.
- φ is the angle of repose of the cantilever.

The third coordinate system is that of the sample. One of the strengths of our method of lateral force calibration is that it is generalized to any surface topography. The

coordinate system must therefore take into account the topography of the sample. This coordinate system makes use of four new unit vectors, which require two separate coordinate rotations:

- $\widehat{k'} = -\sin(\theta)\,\hat{\imath} + 0\hat{\jmath} + \cos(\theta)\hat{k}$ This is the normal $\hat{k}$ unit vector under the first coordinate rotation about the J axis. It is only a transitory unit vector, and does not appear in the derivation except here.
- $\hat{p} = \cos(\theta)\,\hat{\imath} - 0\hat{\jmath} + \sin(\theta)\hat{k}$ This is the unit vector in the plane of the sample, in the direction of the scanner head's movement. The second rotation is around this axis, leading to the formation of the $\hat{n}$ and $\hat{o}$ vectors.
- $\hat{n} = -\cos(\alpha)\sin(\theta)\,\hat{\imath} + \sin(\alpha)\,\hat{\jmath} + \cos(\alpha)\cos(\theta)\hat{k}$ This is the unit vector normal to the surface of the sample.
- $\hat{o} = -\sin(\alpha)\sin(\theta)\,\hat{\imath} - \cos(\alpha)\hat{\jmath} + \sin(\alpha)\cos(\theta)\hat{k}$ This is the unit vector in the plane of the sample, perpendicular to the direction of the scanner head's movement.

The vectors N, O and P are mutually perpendicular. The angles θ and α correspond to the angle of the surface in the I-K and the J-K' planes, respectively.

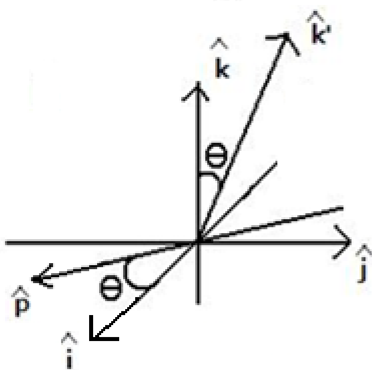

Figure A-3: 1st Rotation about the J axis

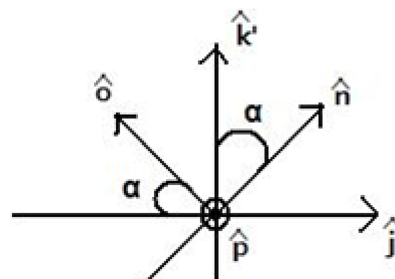

Figure A-4: 2nd Rotation about the P axis

Analysis begins with a free-body diagram of the cantilever tip. There are five forces acting upon the tip in concert; a sixth force, acting in the direction of its long axis, is assumed to be of negligible magnitude.

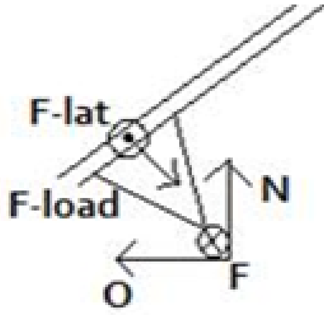

Figure A-5: Forces acting on the cantilever tip

- F_{lat} is the lateral force from the cantilever, which we are solving for. It is equal and opposite to the sum of the x components of the N and O forces.
- F_{load} is the vertical load from the cantilever, which points in the -m direction.
- The force N is the normal force acting on the cantilever, perpendicular to the surface.
- The force O represents any forces in the O plane, parallel to the surface and perpendicular to the P plane.
- The force F is the force of friction at the tip-surface interface, in the P plane.

The lateral force acts in the L direction.

$$\overrightarrow{F_{lat}} = F_{lat} * \hat{\imath} .$$

The load force acts in the -M direction.

$$\overrightarrow{F_{load}} = -F_{load} * \widehat{m} = -F_{load} \left(-\sin(\varphi)\,\hat{\jmath} + \cos(\varphi)\,\hat{k}\right).$$

The O force acts in the IJK directions.

$$\vec{O} = O\hat{O} = O\left(-\sin(\alpha)\sin(\theta)\,\hat{\imath} - \cos(\alpha)\,\hat{\jmath} + \sin(\alpha)\cos(\theta)\,\hat{k}\right).$$

The normal force acts in the N direction indicated on the free-body diagram, and in the I-J-k directions.

$$\vec{N} = N\widehat{N} = N\left(-\cos(\alpha)\sin(\theta)\,\hat{\imath} + \sin(\alpha)\,\hat{\jmath} + \cos(\alpha)\cos(\theta)\,\hat{k}\right).$$

The force of friction acts in the I-K plane.

$$\vec{f} = \mp f\hat{P} = \mp f\left(cos(\theta)\hat{\imath} + sin(\theta)\hat{k}\right).$$

Now, we will separate the forces into their X-Y-Z components. It is at this juncture that we assume that the tip is in equilibrium with the forces acting on it, and furthermore that the equilibrium holds in every direction.

$$\sum F_x = 0 = F_{lat} - \mathrm{O}\sin(\alpha)\sin(\theta) - \mathrm{N}\cos(\alpha)\sin(\theta) \mp f cos(\theta) \quad \text{(A-1)}$$

$$\sum F_y = 0 = -F_{load}\, sin(\varphi) - O cos(\alpha) + \; N sin(\alpha) \quad \text{(A-2)}$$

$$\sum F_z = 0 = -F_{load}\, cos(\varphi) + \mathrm{O}\sin(\alpha)\cos(\theta) + N\cos(\alpha)\cos(\theta) \; \mp f\; sin(\theta) \quad \text{(A-3)}$$

We now solve for the O force by rearranging Eq.2 to yield

$$O = \frac{F_{load}\, sin(\varphi) + N sin(\alpha)}{\cos(\alpha)}$$

We can substitute this value for O into Eq. 3, to obtain the following value for N:

$$N = \frac{F_{load}\;(\cos(\varphi)\cos(\alpha) - \sin(\alpha)\sin(\varphi)\cos(\theta)) \pm f\sin(\theta)\cos(\alpha))}{\cos(\theta)} \; .$$

Substituting these values into Eq. 1 gives us an expression for F_{lat}, the lateral force.

$$F_{lat} =$$

$$F_{load}\;\sin(\theta)\sin(\varphi)\tan(\alpha) +$$

$$\left[F_{load}\left(\frac{\cos(\varphi)\cos(\alpha) - \sin(\varphi)\sin(\alpha)\cos(\theta)}{\cos(\theta)}\right) \pm f tan(\theta)\cos(\alpha)\right](\sin(\alpha)\tan(\alpha) + \cos(\alpha))\sin(\theta) \pm$$

$$f cos(\theta).$$

When we take the average of this equation, we can eliminate the f terms, which relates to the force of friction from the surface-tip interface. Averaging the equation and applying some trigonometric identities yields

$$\overline{F_{lat}} = F_{load}\;\cos(\varphi)\tan(\theta)$$

$$= F_{load_z}\tan(\theta)$$

$$= k_n \Delta z\;\tan(\theta).$$

K_n is the normal force constant and z is the motion of the scanner from zero deflection of the cantilever to the set point. One can also solve for the sum of the x-components of the O and N forces. This result is the negative of the above expression. The purpose of this expression is to find a calibration factor to relate lateral force and average LFM voltage. The lateral force can be rewritten as:

$$F_{lat} = \beta V_{AV-LFM} = k_n \Delta z \tan(\theta) ,$$

where β is the calibration factor. Ideally, a graph of lateral force versus average LFM voltage would be linear, since the calibration factor is a constant:

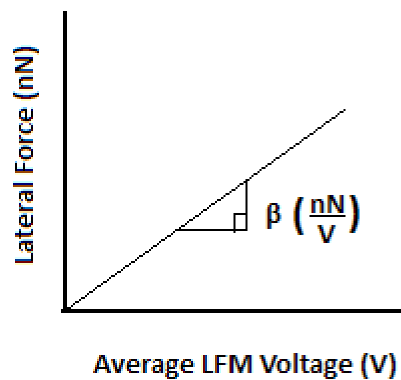

Figure A-6: Graph of Lateral Force versus LFM voltage

One potential flaw of the model is that it might overlook acceleration in the Z direction due to surface topography. The model assumes that the acceleration is close enough to zero that it will not significantly affect the results. We will test that assumption by calculating the typical magnitude of the acceleration.

The force in the Z direction can be expressed as

$$F_z = m\ddot{z}.$$

However, it is convenient for us to express this quantity in the form

$$F_z = m\ddot{z} = m\frac{d}{dt}\left(\frac{dx}{dt}\frac{dz}{dx}\right).$$

In the vertical direction, the cantilever behaves much like a simple harmonic oscillator. Because of this, we can substitute the expression $\frac{k}{\omega^2}$ for the mass, where k is the normal force constant of the cantilever, and ω is the angular frequency. Furthermore, we can replace $\frac{dx}{dt}$ with the more compact V, as this is the expression for velocity. This substitution yields

$$F_z = \frac{k}{\omega^2} V \left(\frac{d}{dt}\frac{dz}{dx}\right).$$

We can now substitute in typical values for the unknowns in the equation. The values chosen are designed to allow us to err on the side of caution; better to estimate too high an acceleration than too low. We will use the following values:

- $K = 1\frac{N}{m}$
- ω = 2π * 10^4rad/sec
- $\frac{dz}{dx} = 1$
- $V = 10^{-4}\frac{m}{s}$
- $\frac{d}{dt} = 1\ Hz$

A unit analysis proves that our values are valid:

$$N = \frac{\frac{N}{m}}{s^{-2}} * \frac{m}{s} * \frac{1}{s} * 1$$

Substituting in the magnitudes of our values gives us the following:

$$m\ddot{z} = \frac{1\ \frac{N}{m}}{(2\pi * 10^4)^2 s^{-2}} * \frac{10^{-4}m}{s} * \frac{1}{s}$$

The force on the cantilever in the Z direction is approximately equal to $\frac{10^{-13}}{4}N$, or 25 femtonewtons. Even at the nanoscale, this is a miniscule force that can be safely ignored in our model.

Appendix B: The Micropipette Puller

The samples used in data collection were borosilicate glass micropipettes, processed using a machine called a micropipette puller. Micropipettes are hollow glass cylinders used for transporting liquid. They are typically a millimeter in diameter, but can reach diameters of a few hundred nanometers when properly processed. Micropipette pullers are commonly found in biology labs, though they also of use to chemists and, to a lesser degree, physicists. The purpose of the puller is, quite literally, to pull; it applies heat and force to the glass micropipettes, stretching them to an extremely fine point.

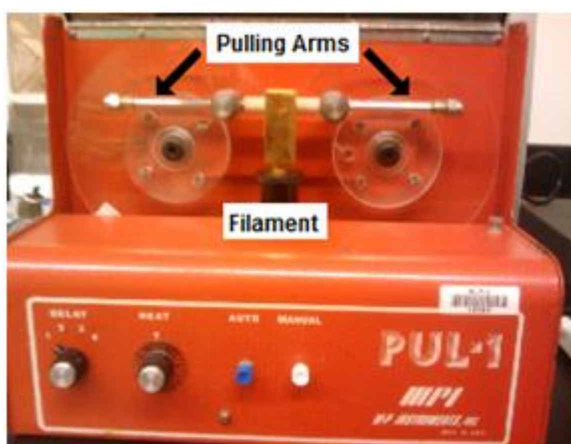

Figure B-1: The WPI PUL-1 Micropipette Puller, care of Professor Gibson, WPI Biotechnology Department

The device has two mechanical arms, with clamps located on opposite sides of the stage, equidistant from a gold plated heating filament colinear with both mechanical arms. Figure 1 shows a diagram of the front of the puller used in this experiment. Use of the device is fairly simple, and falls into the following steps:

1. Unscrew the clamps on both arms and pull them apart, holding them open with one hand.
2. Unscrew the clamp on the right arm and load the right end of the micropipette

into it, using the groove as a guide. Make sure the micropipette is loaded parallel to the surface, as indicated in Fig. 2. Screw down the right clamp snugly.

3. Allow the arms to slowly draw together, and thread the micropipette through the clamp on the left arm. Screw down the left clamp snugly.

When properly loaded, the micropipette should be clamped snugly on either side by the clamps and passing through the middle of the heating filament at an elevation where heating will be even. If the micropipette is loaded either too high or too low, one side of the micropipette will melt faster than the other, causing the tip to break before it can be pulled down to a nanoscale point; such tips usually have diameters on the order of one to ten microns and are thus unsuitable for use in data collection.

Most micropipette pullers have an automatic and a manual mode; others are fully automatic and feature complex computer controls that allow a great deal of control over the pulling process. The device used by WPI is a simpler model, with no computer control but a fairly effective automatic mode and a fully functional manual mode. The device has a system for controlling the power of the heating filament, the force exerted by the pulling bars and the delay between shutting off the power and pulling the micropipettes when operating in automatic mode. The device is pictured in Figure 1.

Two techniques were used to manufacture samples for this experiment's data collection. The first requires a certain level of practice in order to gain a better sense as to how borosilicate glass reacts to the heat of the filament:

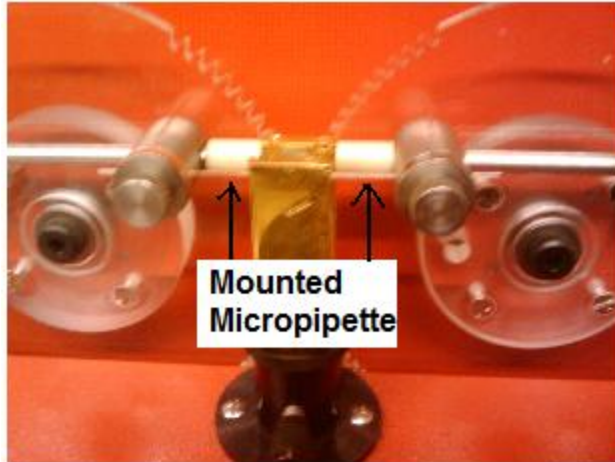

Figure B-2: A micropipette, properly loaded in the micropipette puller

1. Set the heat to a value of seven out of ten.
2. Observe the micropipette carefully while intermittently using the manual function to heat the filament.
3. Stop heating the filament once the micropipette begins to accelerate apart quickly. Allow the micropipette to cool for a few seconds. Repeat.

The technique has a high error rate, as too much heat can cause the tube to pull too quickly, producing bell shaped tips that are useless for research. Properly executed, however, the technique produces excellent samples.

A less controlled technique for sample manufacture is simply to set the heat at its maximum value and keep the filament on until the micropipette melts. This technique creates samples with a range of qualities, from poor to suitable, and is best for use when time is scarce or the experimenter is inexperienced with the first technique.